

Artificial Interference Aided Physical Layer Security in Cache-enabled Heterogeneous Networks

Wu Zhao, Zhiyong Chen, Kuikui Li, and Bin Xia

Cooperative Medianet Innovation Center, Shanghai Jiao Tong University, Shanghai, P. R. China

Email: {zhaowu,zhiyongchen,kuikuili,bxia}@sjtu.edu.cn

Abstract—Caching popular contents is a promising way to offload the mobile data traffic in wireless networks, but so far the potential advantage of caching in improving physical layer security (PLS) is rarely considered. In this paper, we contribute to the design and theoretical understanding of exploiting the caching ability of users to improve the PLS in a wireless heterogeneous network (HetNet). In such network, the base station (BS) ensures the secrecy of communication by utilizing some of the available power to transmit a pre-cached file, such that only the eavesdropper's channel is degraded. Accordingly, the node locations of BSs, users and eavesdroppers are first modeled as mutually independent poisson point processes (PPPs) and the corresponding file access protocol is developed. We then derive analytical expressions of two metrics, average secrecy rate and secrecy coverage probability, for the proposed system. Numerical results are provided to show the significant security advantages of the proposed network and to characterize the impact of network resource on the secrecy metrics.

I. INTRODUCTION

With the thriving development of mobile paying and internet of things, the privacy and security of wireless communication networks have become one of the most important issues. However, the broadcast nature of wireless channel leads to severe security vulnerabilities such as eavesdropping and jamming [1]. To overcome these shortages, physical layer security (PLS) has emerged as a promising technology to complement and augment the security of wireless networks.

In [2], Wyner shows that when the eavesdropping channel is degraded than the main legitimating channel, the secrecy of communication can be perfectly guaranteed at a non-zero rate. And first, characterizes the maximal achievable secrecy rate as 'secrecy capacity' of the discrete wiretap channel. Further, various efficient approaches are proposed to improve the secrecy capacity, e.g., artificial noise adding [3], and relay cooperating [4]. By exploiting multi-input single-output techniques, [3] proposes an artificial noise assisted beamforming scheme, which imposes the artificial noise into the null space of the legitimating channel to degrade the eavesdropping channel. One source-destination pair with multiple relays intercepted by multiple eavesdroppers (ERs) is considered in [4]. By determining the relay weights, the authors maximize the achievable secrecy rate under different cooperating schemes.

With the popularization of and explosion of small communication equipments, the topology of the wireless network is becoming densely and randomly, which intensifies the concern for secure transmission. Based on poisson point process (PPP) [5], [6]–[9] propose various schemes to improve physical layer

security in such wireless heterogeneous network (HetNet). In [6], the authors consider two transmission strategies based on sectoring and beamforming with artificial noise aided and investigate the secrecy capacity of both schemes. By exchanging the location information between BSs, [7] analysis the effect of node locations on the achievable secrecy rate. In [8], the authors develop a tractable framework to analysis the average secrecy rate in a three-tier sensor network consisting of sensors, access points and sinks. [9] confound ERs with jamming signal from friendly jammers and artificial noise from full-duplex user. By selecting the jammer selection threshold to maximize secrecy probability.

Recently, caching popular contents at base station (BSs) and users has been introduced as a promising technique to address the mobile data tsunami in wireless networks [10], [11]. The authors in [12] propose centralized and decentralized caching algorithms to guarantee secret transmission rate by coded multicast delivery. Further, [13] utilizes the cached files of users as side information to cancel received interference from. However, the potential of caching in improving physical layer security is rarely considered until recently [14]. The authors study the secure cooperative transmission among multiple cache-enabled BSs with the shared video data. Under the secrecy rate constraint, the total transmit power is minimized by jointly optimizing caching and transmission policies.

In this paper, we propose a heuristic scheme to enhance physical layer security in a cache-enabled HetNet by exploiting the caching ability of users. Instead of sending Gaussian noise as [3], [6], the BS transmits the target message combined with an artificial interference which is a file pre-cached at user. Since the cached file is known perfectly by the user, this part of interference can be erased as [13] while [3] and [6] need the orthogonal space of legitimating channel to isolate noise. Meanwhile, ERs are confused by this part of artificial interference due to absence of this file. Specifically, by using stochastic geometry, we model the node locations (BSs, users and ERs) of the three-tier HetNet as mutually independent PPPs. The file access protocol is then proposed based on whether the file is cached or not and whether the user has cache ability or not. Accordingly, we derive analytical expressions of average secrecy rate and secrecy coverage probability for the proposed system in different transmission schemes. Numerical results show that proposed scheme can achieve promising performance in the both ER-dense and ER-sparse scenarios.

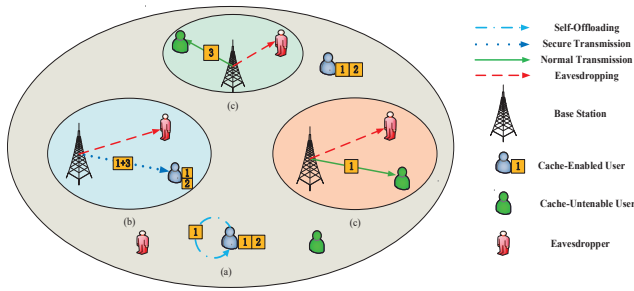


Fig. 1. System model of wireless cache-enabled heterogeneous networks with eavesdroppers, where (a), (b) and (c) stand of Self-offloading, Secure-transmission and Normal-transmission, respectively.

II. SYSTEM MODEL

A. Network Structure

As shown in Fig. 1, we consider a general wireless cache-enabled HetNet consisting three tiers of BSs, users and ERs, where the locations of BSs, users and ERs in each tier are spatially distributed based on independent PPPs, denoted as Φ_b , Φ_u and Φ_e with density λ_b , λ_u and λ_e , respectively. All nodes operate in single-antenna and we consider the downlink transmission, where time is divided into discrete slots with equal duration and we study one slot of the system. Large-scale fading and small-scale fading are both considered. We use $d^{-\beta}$ to denote large scale fading along the distance d , where $2 \leq \beta \leq 4$ is the path-loss exponent. For the small-scale fading, we consider the Rayleigh fading channel h , i.e., $|h|^2 \sim \exp(1)$.

Consider a file library consisting of N files denoted by $\mathcal{F} \triangleq \{f_1, f_2, \dots, f_N\}$, and all the files are assumed to have equal length L . Each user randomly requests a file f_i with probability p_i and $\sum_{i=1}^N p_i = 1$. Without loss of generality (w.l.o.g), we assume $p_1 \geq p_2 \geq \dots \geq p_N$. Here, we also consider a file can only be stored entirely rather than partially. Non-colluding ERs intercept information by passive listening signal from BS.

We assume only α part of users have cache ability, where $0 \leq \alpha \leq 1$. The cache-enabled users also follow a thinning PPP with density $\alpha\lambda_u$. The cache-enabled users have same caching size with $(M \times L)$ bits, where $M < N$ and cache the same M -most popular files out of \mathcal{F} in this paper, which are marked as set $\mathcal{M} \triangleq \{f_1, f_2, \dots, f_M\}$. To the aim of tractability, we assume that BSs can access all the files in \mathcal{F} by directly connect to the core-network and neglect the extra cost for BS to fetch files. The set \mathcal{M} will be broadcasted to all users by BSs at off-peak time then pre-stored at cache-enabled users. ERs considered in this paper have no cache ability.

B. File Access Protocol

Let Q be the total amount of request from users in Φ_u at one slot. As indicated in Fig. 1, the file access protocol can be described as follows:

- (a) **Self-offloading:** When a cache-enabled user happens to request a file in \mathcal{M} , the request will be satisfied

and offloaded immediately from the user's local storage, termed as "Self-offloading". By denoting the cache hit probability of the request fall in \mathcal{M} as $\delta = \sum_{i=1}^M p_i$, the amount of this request is $Q_{SO} = \alpha\delta Q$.

- (b) **Secure-transmission:** When a cache-enabled user requests f_i ($i > M$) from the complementary set $\mathcal{F} \setminus \mathcal{M}$ which is denoted as $\mathcal{C} \triangleq \{f_{M+1}, f_{M+2}, \dots, f_N\}$, the target file f_i can be provided by the nearest BS. In order to improve the transmission security, BS can combine the target file f_i with a cached file f_m , i.e., $f_m \in \mathcal{M}$.¹ Therefore, the transmission signal is $t_i = \sqrt{\theta P}x_i + \sqrt{(1-\theta)P}x_m$, where P is the transmission power of BS, x_i and x_m are the signal of f_i and f_m with $E(|x_i|^2) = E(|x_m|^2) = 1$ respectively, and $\theta \in (0, 1]$ is the ratio of power allocation.

Since the pre-cached signal x_m is known perfectly by the cache-enabled user, the user can cancel the extra interference x_m . However, x_m is unknown for the ERs and thus can be viewed as a interference. We term this transmission as "Secure-transmission". And the amount of this request is $Q_{ST} = \alpha(1-\delta)Q$

- (c) **Normal-transmission:** When a user does not have cache ability and requests f_i from \mathcal{F} , f_i will be transmitted by its nearest BS, termed as "Normal-transmission". The transmission signal is $t_i = \sqrt{P}x_i$. Moreover, according to which subset of f_i belongs to, the request can be divided into two types: $f_i \in \mathcal{M}$ and $f_i \in \mathcal{C}$. Therefore the amount of these two types request are $Q_{NT\mathcal{M}} = (1-\alpha)\delta Q$, $Q_{NT\mathcal{C}} = (1-\alpha)(1-\delta)Q$, respectively.

In this paper, we assume all the BSs work in the full loaded state due to $\lambda_u \gg \lambda_b$ and each BS randomly serve one of user requests with equal probability. Therefore, the locations of BS in different states $\{(b), (c)\}$ are distributed as thinning PPPs $\Phi_{b_1}, \Phi_{b_2}, \Phi_{b_3}$ with density $\lambda_{b_1} = \frac{Q_{ST}}{Q_{ST}+Q_{NT}}\lambda_b = \frac{\alpha(1-\delta)}{1-\alpha\delta}\lambda_b$, $\lambda_{b_2} = \frac{Q_{NT\mathcal{M}}}{Q_{ST}+Q_{NT}}\lambda_b = \frac{(1-\alpha)\delta}{1-\alpha\delta}\lambda_b$ and $\lambda_{b_3} = \frac{Q_{NT\mathcal{C}}}{Q_{ST}+Q_{NT}}\lambda_b = \frac{(1-\alpha)(1-\delta)}{1-\alpha\delta}\lambda_b$ respectively.

III. ANALYSIS OF TRANSMISSION PROTOCOL

According to Slivnyak's theorem [15], a typical user u_0 locating at the origin of the Euclidean area does not change the distribution of PPP, no matter with or without caching ability. We also consider that the link between u_0 and its serving BS b_0 can be eavesdropped by all ERs in the network.

A. Normal Transmission

A typical user with no cache ability denoted as u_0 requests f_i from \mathcal{F} . The nearest BS b_0 serves this request within the normal-transmission. Since the interference signals transmitted by other BSs from $\Phi_{b_1}, \Phi_{b_2}, \Phi_{b_3}$ cannot be cancelled without cached files, the interference u_0 suffering is equivalent com-

¹W.l.o.g, we use f_1 as f_m in this paper which is noticed to all cache-enabled users.

ing from $\{\Phi_b \setminus b_0\}$ with power P . Therefore the received signal of un_0 is

$$y_{un_0} = \sqrt{P} d_{un_0, b_0}^{-\frac{\beta}{2}} h_{un_0, b_0} x_i + \sum_{k \in \{\Phi_b \setminus b_0\}} \sqrt{P} d_{un_0, b_k}^{-\frac{\beta}{2}} h_{un_0, b_k} x_{k'} + n_0, \quad (1)$$

where d_{un_0, b_0} denotes the distance between un_0 and b_0 , h_{un_0, b_0} (h_{un_0, b_k}) represents the Rayleigh fading channel between un_0 and b_0 (b_k), x_i ($x_{k'}$) is the transmission signal of b_0 (b_k), and $n_0 \sim \mathcal{CN}(0, \sigma^2)$ denotes the additive white Gaussian noise (AWGN). W.l.o.g, the variance of AWGN noise n_i is σ^2 for $i = 0, 1, 2, 3$ in this paper.

Therefore the received signal-to-interference-plus-noise ratio (SINR) at un_0 is

$$SINR_{un_0} = \frac{P d_{un_0, b_0}^{-\beta} |h_{un_0, b_0}|^2}{\sum_{k \in \{\Phi_b \setminus b_0\}} P d_{un_0, b_k}^{-\beta} |h_{un_0, b_k}|^2 + \sigma^2}. \quad (2)$$

For the ER of un_0 , the received signal at an arbitrary ER $e_j \in \Phi_e$ is similarly given by:

$$y_{e_j n} = \sqrt{P} d_{e_j, b_0}^{-\frac{\beta}{2}} h_{e_j, b_0} x_i + \sum_{k \in \{\Phi_b \setminus b_0\}} \sqrt{P} d_{e_j, b_k}^{-\frac{\beta}{2}} h_{e_j, b_k} x_{k'} + n_1. \quad (3)$$

Because x_i is eavesdropped signal for e_j , the SINR of e_j can be written as

$$SINR_{e_j n} = \frac{P d_{e_j, b_0}^{-\beta} |h_{e_j, b_0}|^2}{\sum_{k \in \{\Phi_b \setminus b_0\}} P d_{e_j, b_k}^{-\beta} |h_{e_j, b_k}|^2 + \sigma^2}. \quad (4)$$

B. Secure Transmission

A typical user with cache ability denoted as uc_0 requests f_i from \mathcal{C} . The nearest BS b_0 will serve this request within the secure-transmission. The received signal at uc_0 is given by:

$$\begin{aligned} y_{uc_0} &= \sqrt{\theta P} d_{uc_0, b_0}^{-\frac{\beta}{2}} h_{uc_0, b_0} x_i + \sqrt{(1-\theta)P} d_{uc_0, b_0}^{-\frac{\beta}{2}} h_{uc_0, b_0} x_m \\ &+ \sum_{j \in \{\Phi_{b_1} \setminus b_0\}} \left\{ \sqrt{\theta P} d_{uc_0, b_j}^{-\frac{\beta}{2}} h_{uc_0, b_j} x_j + \sqrt{(1-\theta)P} d_{uc_0, b_j}^{-\frac{\beta}{2}} h_{uc_0, b_j} x_m \right\} \\ &+ \sum_{k \in \Phi_{b_2}} \sqrt{P} d_{uc_0, b_k}^{-\frac{\beta}{2}} h_{uc_0, b_k} x_k + \sum_{l \in \Phi_{b_3}} \sqrt{P} d_{uc_0, b_l}^{-\frac{\beta}{2}} h_{uc_0, b_l} x_l + n_2. \end{aligned} \quad (5)$$

As described in Section II-B, the pre-cached signal x_m is known perfectly at uc_0 . And assume that the perfect channel state information (CSI) is fully available at cache-enabled users. Therefore, the $(1-\theta)$ part of interference from Φ_{b_1} and fully interference from Φ_{b_2} can be cancelled [13]. The SINR of uc_0 is

$$SINR_{uc_0} = \frac{\theta P d_{uc_0, b_0}^{-\beta} |h_{uc_0, b_0}|^2}{\underbrace{\theta P \sum_{j \in \{\Phi_{b_1} \setminus b_0\}} d_{uc_0, b_j}^{-\beta} |h_{uc_0, b_j}|^2}_{I_{\Phi_{b_1}}} + \underbrace{P \sum_{l \in \Phi_{b_3}} d_{uc_0, b_l}^{-\beta} |h_{uc_0, b_l}|^2}_{I_{\Phi_{b_3}}} + \sigma^2}. \quad (6)$$

²Note that $x_{k'}$ include secure transmission and normal transmission from BSs in $\{\Phi_b \setminus b_0\}$.

For the ER of uc_0 , the received signal $y_{e_j c}$ is given by

$$\begin{aligned} y_{e_j c} &= \sqrt{\theta P} d_{e_j, b_0}^{-\frac{\beta}{2}} h_{e_j, b_0} x_i + \sqrt{(1-\theta)P} d_{e_j, b_0}^{-\frac{\beta}{2}} h_{e_j, b_0} x_m \\ &+ \sum_{k \in \{\Phi_b \setminus b_0\}} \sqrt{P} d_{e_j, b_k}^{-\frac{\beta}{2}} h_{e_j, b_k} x_{k'} + n_3, \end{aligned} \quad (7)$$

Thus the SINR of e_j can be calculated as

$$SINR_{e_j c} = \frac{\theta P |h_{e_j, b_0}|^2 d_{e_j, b_0}^{-\beta}}{P \underbrace{\sum_{k \in \{\Phi_b \setminus b_0\}} d_{e_j, b_k}^{-\beta} |h_{e_j, b_k}|^2}_{I_{\Phi_b}} + (1-\theta) P d_{e_j, b_0}^{-\beta} |h_{e_j, b_0}|^2 + \sigma^2}. \quad (8)$$

Remark 1. We can observe from (8) that the expression has the form of $\frac{\theta X}{C + (1-\theta)X}$, where $X = P |h_{e_j, b_0}|^2 d_{e_j, b_0}^{-\beta}$ which is a function of variables h_{e_j, b_0} and d_{e_j, b_0} , while $C = P I_{\Phi_b} + \sigma^2$ is not relevant. Therefore we have $SINR_{e_j c} \leq \frac{\theta}{1-\theta} \triangleq \gamma_{th_0}$.

IV. SECURITY METRICS ANALYSIS

In this section, the secrecy performance of two transmission protocols are compared in terms of average secrecy rate and secrecy coverage probability.

A. Average Secrecy Rate

Consider a link between the user u_0 and serving BS b_0 being intercepted by $ER \in \Phi_e$. We focus on the most detrimental ER which has the highest receive SINR from b_0 .

The instantaneous secrecy rate \mathcal{C} is thus given as

$$\mathcal{C} \triangleq [C_u - C_e]^\dagger, \quad (9)$$

where $[x]^\dagger = \max\{x, 0\}$. C_u and C_e are, respectively, the instantaneous capacity of the user's (u_0) channel and the most detrimental ER's channel, which can be expressed uniformly as $C_i = \log_2(1 + \gamma_i)$, $i = u, e$. Here, γ_e is the instantaneous received SINR of the most detrimental ER, which is given by

$$\gamma_e = \max_{e_j \in \Phi_e} \{SINR_{e_j}\}. \quad (10)$$

The average secrecy rate is defined as

$$\bar{\mathcal{C}} \triangleq \int_0^\infty \int_0^\infty [C_u - C_e]^\dagger d\gamma_u d\gamma_e, \quad (11)$$

and can be rewritten as [8]

$$\bar{\mathcal{C}} = \frac{1}{\ln 2} \int_0^\infty [1 - F_{\gamma_u}(\gamma_{th})] \frac{F_{\gamma_e}(\gamma_{th})}{1 + \gamma_{th}} d\gamma_{th}, \quad (12)$$

where F_{γ_u} and (F_{γ_e}) are the cumulative probability functions (CDFs) of γ_u and (γ_e) , respectively. Therefore, the $\bar{\mathcal{C}}$ of two transmission protocols are given as follow.

1) *Secure Transmission:*

Lemma 1. Let γ_{uc} be the SINR of the typical user with cache ability, the CDF of γ_{uc} can be calculated as

$$F_{\gamma_{uc}}(\gamma_{th}) = 1 - 2\pi\lambda_b \int_0^\infty x \exp\left\{-\pi x^2 \left[\mathcal{Z}(\gamma_{th})\lambda_{b_1} + \mathcal{Z}\left(\frac{\gamma_{th}}{\theta}\right)\lambda_{b_3} + \lambda_b \right] - \frac{\sigma^2}{\theta P} \gamma_{th} x^\beta \right\} dx, \quad (13)$$

where $\mathcal{Z}(\gamma_{th}) = \frac{2\gamma_{th}}{\beta-2} {}_2F_1[1, 1 - \frac{2}{\beta}; 2 - \frac{2}{\beta}; -\gamma_{th}]$, ${}_2F_1[\cdot]$ is the Gauss hypergeometric function.

Proof. Please refer to Appendix A. \square

Lemma 2. Let γ_{ec} be the SINR of the most detrimental ER of the typical cache-enabled user, the CDF of γ_{ec} is written as

$$F_{\gamma_{ec}}(\gamma_{th}) = \begin{cases} \tilde{F}_{\gamma_{ec}}(\gamma_{th}) & 0 \leq \gamma_{th} \leq \gamma_{th_0} \\ 1 & \text{else,} \end{cases} \quad (14)$$

where $\tilde{F}_{\gamma_{ec}}(\gamma_{th})$ is

$$\exp\left\{-2\pi\lambda_e \int_0^\infty x \exp\left\{-\pi\lambda_b \Gamma\left(1 + \frac{2}{\beta}\right) \Gamma\left(1 - \frac{2}{\beta}\right) \left[\frac{\gamma_{th} x^\beta}{\theta - (1-\theta)\gamma_{th}} \right]^{\frac{2}{\beta}} - \frac{\sigma^2}{P} \left[\frac{\gamma_{th} x^\beta}{\theta - (1-\theta)\gamma_{th}} \right] \right\} dx \right\}. \quad (15)$$

and $\Gamma[\cdot]$ is the Gamma function.

Proof. Please refer to Appendix B. \square

Theorem 1. In the interference-limited scenario, the average secrecy rate for the secure transmission is given by

$$\bar{C}_{ST} = \frac{1}{\ln 2} \int_0^{\gamma_{th_0}} \frac{\exp\left\{-\frac{\lambda_e}{\lambda_b} / \Gamma\left(1 + \frac{2}{\beta}\right) \Gamma\left(1 - \frac{2}{\beta}\right) \left[\frac{\gamma_{th}}{\theta - (1-\theta)\gamma_{th}} \right]^{\frac{2}{\beta}} \right\}}{(1 + \gamma_{th}) \left[\mathcal{Z}(\gamma_{th}) \frac{\lambda_{b_1}}{\lambda_b} + \mathcal{Z}\left(\frac{\gamma_{th}}{\theta}\right) \frac{\lambda_{b_3}}{\lambda_b} + 1 \right]} d\gamma_{th} + \frac{1}{\ln 2} \int_{\gamma_{th_0}}^\infty \frac{d\gamma_{th}}{(1 + \gamma_{th}) \left[\mathcal{Z}(\gamma_{th}) \frac{\lambda_{b_1}}{\lambda_b} + \mathcal{Z}\left(\frac{\gamma_{th}}{\theta}\right) \frac{\lambda_{b_3}}{\lambda_b} + 1 \right]}. \quad (16)$$

Proof. By substituting (13) and (14) into (12), it is easy to obtain this theorem. \square

2) *Normal Transmission:*

Lemma 3. Let γ_{un} as the SINR of the typical user without cache ability. Similar to (13), the CDF of γ_{un} is

$$F_{\gamma_{un}}(\gamma_{th}) = 1 - 2\pi\lambda_b \int_0^\infty x \exp\left[-\pi\lambda_b x^2 (\mathcal{Z}(\gamma_{th}) + 1) - \frac{\sigma^2}{P} \gamma_{th} x^\beta \right] dx. \quad (17)$$

Lemma 4. Let γ_{en} as the SINR of the most detrimental ER of the typical user without cache ability. Similar to (14), it is easy to obtain the CDF of γ_{en} , which is given by

$$F_{\gamma_{en}}(\gamma_{th}) = \exp\left\{-2\pi\lambda_e \int_0^\infty x \exp\left\{-\pi\lambda_b \Gamma\left(1 + \frac{2}{\beta}\right) \Gamma\left(1 - \frac{2}{\beta}\right) \left[\gamma_{th} x^\beta \right]^{\frac{2}{\beta}} - \frac{\sigma^2}{P} \gamma_{th} x^\beta \right\} dx \right\}. \quad (18)$$

Theorem 2. In the interference-limited scenario, the average secrecy rate for the normal transmission is derived as

$$\bar{C}_{NT} = \frac{1}{\ln 2} \int_0^\infty \frac{\exp\left\{-\frac{\lambda_e}{\lambda_b} / \Gamma\left(1 + \frac{2}{\beta}\right) \Gamma\left(1 - \frac{2}{\beta}\right) \gamma_{th}^{\frac{2}{\beta}} \right\}}{(1 + \gamma_{th}) [\mathcal{Z}(\gamma_{th}) + 1]} d\gamma_{th}. \quad (19)$$

Proof. By substituting (17) and (18) into (12), we obtain this theorem. \square

By comparing (16) and (19), we can find that \bar{C}_{ST} and \bar{C}_{NT} are both dependent on λ_e/λ_b , while \bar{C}_{ST} is also dependent on the power allocation ratio θ and the ratio of BS in three different states λ_{b_i}/λ_b , $i = 1, 3$. Note that λ_{b_i}/λ_b , $i = 1, 3$, are related to the cache-user ratio α and the cache hit ratio δ . Numerical results will be given in Section V to show the effects of these parameters.

B. *Secrecy Coverage Probability*

Let R_s be a given secrecy rate threshold. The delivery is securely successful when the instantaneous secrecy rate \mathcal{C} is larger than the threshold R_s . Thus, the secrecy coverage probability can be expressed as

$$\begin{aligned} \mathcal{P} &\triangleq P_r(\mathcal{C} > R_s) = P_r[\log_2(1 + \gamma_u) - \log_2(1 + \gamma_e) > R_s] \\ &= \mathbb{E}_{\gamma_u, \gamma_e} \left\{ \mathbf{1}_{[\gamma_u > (1 + \gamma_e) 2^{R_s} - 1]} \right\} \\ &= \int_0^\infty \int_{(1 + \gamma_e) 2^{R_s} - 1}^\infty f_{\gamma_u}(\gamma_1) f_{\gamma_e}(\gamma_2) d\gamma_1 d\gamma_2 \\ &= \int_0^\infty f_{\gamma_e}(\gamma_{th}) \{1 - F_{\gamma_u}[2^{R_s}(1 + \gamma_{th}) - 1]\} d\gamma_{th}, \end{aligned} \quad (20)$$

where $f_{\gamma_u}(\gamma_u)$ and $f_{\gamma_e}(\gamma_e)$ are the probability distribution functions (PDFs) of γ_u and γ_e , respectively.

Theorem 3. In the interference-limited scenario with the secure transmission, the secrecy coverage probability is

$$\mathcal{P}_{ST} = \int_0^{\gamma_{th_0}} \left\{ \frac{\exp\left[-\frac{\lambda_e}{\lambda_b} / \Gamma\left(1 + \frac{2}{\beta}\right) \Gamma\left(1 - \frac{2}{\beta}\right) \left[\frac{\gamma_{th}}{\theta - (1-\theta)\gamma_{th}} \right]^{\frac{2}{\beta}} \right]}{\mathcal{G}(\gamma_{th}) \frac{\lambda_{b_1}}{\lambda_b} + \mathcal{G}\left(\frac{\gamma_{th}}{\theta}\right) \frac{\lambda_{b_3}}{\lambda_b} + 1} \frac{2\lambda_e \theta \gamma_{th}^{-\frac{\beta+2}{\beta}}}{\beta \lambda_b \Gamma\left(1 + \frac{2}{\beta}\right) \Gamma\left(1 - \frac{2}{\beta}\right) \left[\frac{\gamma_{th}}{\theta - (1-\theta)\gamma_{th}} \right]^{\frac{\beta-2}{\beta}}} \right\} d\gamma_{th}, \quad (21)$$

where $\mathcal{G}(\gamma_{th})$ is given as

$$\mathcal{G}(\gamma_{th}) = [(1 + \gamma_{th}) 2^{R_s} - 1]^{\frac{2}{\beta}} \int_{[(1 + \gamma_{th}) 2^{R_s} - 1]^{\frac{2}{\beta}}}^\infty \frac{1}{1 + x^{\frac{\beta}{2}}} dx. \quad (22)$$

Proof. By differentiating (14) to get $f_{\gamma_e}(\gamma_e)$, then substituting $f_{\gamma_e}(\gamma_e)$ and (13) into (20), we obtain this theorem. \square

Theorem 4. In the interference-limited scenario with the normal transmission, the secrecy coverage probability is

$$\mathcal{P}_{NT} = \int_0^\infty \left\{ \frac{\exp\left[-\frac{\lambda_e}{\lambda_b} / \Gamma\left(1 + \frac{2}{\beta}\right) \Gamma\left(1 - \frac{2}{\beta}\right) \gamma_{th}^{\frac{2}{\beta}} \right]}{\mathcal{G}(\gamma_{th}) + 1} \frac{2\lambda_e \gamma_{th}^{-\frac{\beta+2}{\beta}}}{\beta \lambda_b \Gamma\left(1 + \frac{2}{\beta}\right) \Gamma\left(1 - \frac{2}{\beta}\right)} \right\} d\gamma_{th} \quad (23)$$

Proof. By differentiating (18) to get $f_{\gamma_e}(\gamma_e)$, then substituting $f_{\gamma_e}(\gamma_e)$ and (17) into (20), we get this theorem. \square

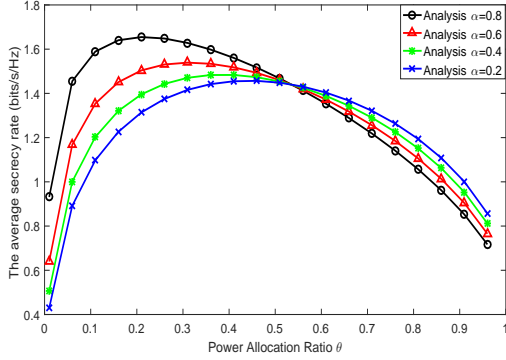


Fig. 2. The average secrecy rate \bar{C}_{ST} v.s. power allocation ratio θ

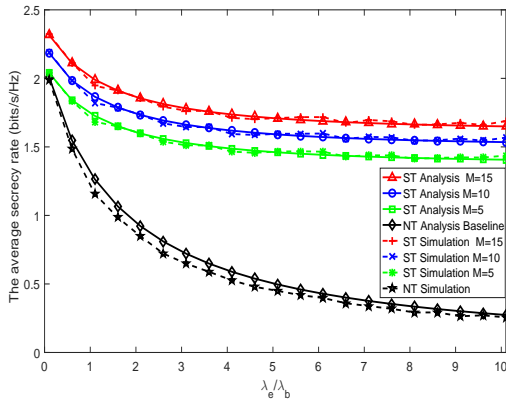


Fig. 3. The average secrecy rate \bar{C} v.s. λ_e/λ_b

V. NUMERICAL RESULTS

In this section, numerical results are provided to evaluate the performance of the proposed transmission schemes. The BSs, ERs and users are distributed based on PPPs with density $\{\lambda_b, \lambda_e, \lambda_u\} = \{1, 5, 100\}/km^2$ in the simulation. We consider the transmission power $P = 30$ dBm and the noise power $\sigma^2 = -174$ dBm. We consider the path loss exponent $\beta = 4$, the total number of files $N = 100$, the cache size $M = 5$, the power allocation ratio $\theta = 0.5$, and the cache user ratio $\alpha = 0.5$. In the simulation, the file popularity distribution is modeled as Zipf distribution, i.e., the requested probability of the i -th ranked file is given by $p_i = \frac{1/i^\eta}{\sum_{j=1}^N 1/j^\eta}$ where $\eta \geq 0$ characterizes the skew of the popularity distribution. We use $\eta = 0.8$ in the simulation. These parameters will not change unless specified otherwise.

In Fig.2, the average secrecy rate of the secure transmission \bar{C}_{ST} versus the power allocation ratio θ is illustrated. It can be seen that there exists an optimal θ^* to achieve the maximal \bar{C}_{ST} for a given α , and different α has different θ^* . As presented in (16), \bar{C}_{ST} cannot be expressed in a closed form. As such, we cannot derive θ^* in theory. We can observe that the average secrecy rate \bar{C}_{ST} first increase with θ when $\theta \in (0, \theta^*)$, then decreases with θ when $\theta \in (\theta^*, 1)$. This

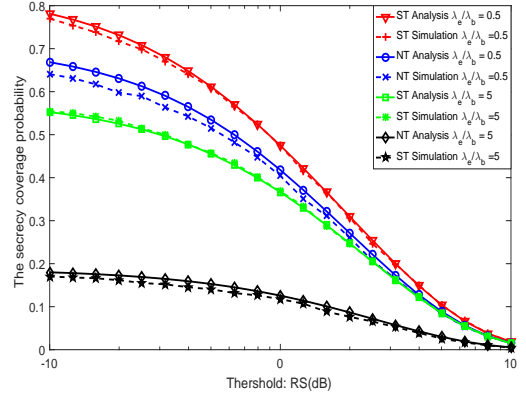


Fig. 4. The secrecy coverage probability vs. threshold

interesting phenomenon can be well explained from (6) and (8). The increase of θ improves the SINRs of both user and ER, but the increment at user is dominant in $(0, \theta^*)$. When θ is getting larger, the \bar{C}_{ST} will be compromised due to the growing effects of eavesdropping. We can also obtain that the secure transmission can achieve better optimal \bar{C} in larger α scenario, because more secure transmissions occurs in the network.

In Fig.3, the average secrecy rate \bar{C} versus the density ratio of $\frac{\lambda_e}{\lambda_b}$ with different cache size M is illustrated. Note from (19) that \bar{C}_{NT} is only depend on $\frac{\lambda_e}{\lambda_b}$ which is considered as a baseline. We can see that with the increase of $\frac{\lambda_e}{\lambda_b}$, the \bar{C} is decreased for both with and without cache-enabled transmission schemes, which indicates that more ERs cause more serious eavesdropping. It should be highlighted that, even with $\frac{\lambda_e}{\lambda_b} = 10$, the \bar{C}_{ST} is still above 1.5 bits/s/Hz which only reduced 25% from above 2 bits/s/Hz when $\frac{\lambda_e}{\lambda_b} = 0.1$, while \bar{C}_{NT} reduces to 0.3 bits/s/Hz from 2 bits/s/Hz, i.e., reduced by 85%. In addition, we can also observe that the \bar{C}_{ST} improves with increasing cache size M , due to more interference signal can be cancelled with larger ratio of Φ_{b_1} and Φ_{b_2} .

In Fig.4, the secrecy coverage probability \mathcal{P} for various $\frac{\lambda_e}{\lambda_b}$ is presented. We can observe that \mathcal{P}_{ST} is much higher than \mathcal{P}_{NT} for both $\frac{\lambda_e}{\lambda_b} = 5$ and 0.5, which indicates the promising effect of secure transmission in both ER-dense scenario and ER-sparse scenario. Similar as Fig.3, we can also see that more ERs cause more serious eavesdropping leading lower secrecy coverage probability. The simulation results are presented along with the theoretical ones in Fig.3 and Fig. 4. We can see from the figures that the theoretical results are in excellent agreement with the simulation results.

VI. CONCLUSION

In this paper, we reveal that the caching ability of users can be used to improve the transmission security for physical layer security in the wireless cache-enabled HetNet. The corresponding secure transmission scheme is developed, where the transmitter combines the message signal with the pre-cached file. This scheme can introduce extra interference at ER, but this interference can be cancelled at the cache-enabled

users. Based on stochastic geometry, we derive the expression of average secrecy rate and secrecy coverage probability for the secure transmission and the normal transmission. Finally, we show that the secure transmission achieves a significant security gain than the normal transmission.

APPENDIX

A. Proof of Lemma 1

By replacing the distance d_{u_0, b_0} between the typical user and its nearest BS with x , the PDF of x is $f_X(x) = 2\pi\lambda_b x \exp\{-\pi\lambda_b x^2\}$ [5]. Then the CDF of γ_{uc} is derived as

$$\begin{aligned} F_{\gamma_{uc}}(\gamma_{th}) &\triangleq P_r[SINR_{uc} \leq \gamma_{th}] = \mathbb{E}_x[SINR_{uc} \leq \gamma_{th} | d_{u_0, b_0} = x] \\ &= \int_0^{+\infty} P_r\left[\frac{\theta P |h_{u_0, b_0}|^2 x^{-\beta}}{\theta P I_{\Phi_{b_1}} + P I_{\Phi_{b_3}} + \sigma^2} \leq \gamma_{th}\right] f_X(x) dx \\ &= \int_0^{+\infty} P_r\left[|h_{u_0, b_0}|^2 \leq \gamma_{th} x^\beta (I_{\Phi_{b_1}} + \frac{I_{\Phi_{b_3}}}{\theta} + \frac{\sigma^2}{\theta P})\right] f_X(x) dx \\ &\stackrel{(a)}{=} 1 - \int_0^{+\infty} \mathcal{L}_{I_{\Phi_{b_1}}}(\gamma_{th} x^\beta) \mathcal{L}_{I_{\Phi_{b_3}}}\left(\frac{\gamma_{th} x^\beta}{\theta}\right) e^{-\frac{\gamma_{th} x^\beta \sigma^2}{\theta P}} f_X(x) dx, \quad (24) \end{aligned}$$

where Step (a) follows from $|h_{u_0, b_0}|^2 \sim \exp(1)$. Under the condition of $d_{u_0, b_0} = x$, the remaining interferences resulted from Φ_{b_1} and Φ_{b_3} are spatially located at the outside of the circle centered at u_0 with radius x denoted as $\mathcal{C}_{(u_0, x)}$. Therefore the Laplace transform $\mathcal{L}_{I_{\Phi_{b_1}}}$ is derived as

$$\begin{aligned} \mathcal{L}_{I_{\Phi_{b_1}}}[\gamma_{th} x^\beta] &= \mathbb{E}_{I_{\Phi_{b_1}}}\left[\exp(-\gamma_{th} x^\beta \sum_{j \in \{\Phi_{b_1} \setminus b_0\}} d_{u_0, b_j}^{-\beta} |h_{u_0, b_j}|^2)\right] \\ &= \mathbb{E}_{I_{\Phi_{b_1}}}\left\{\prod_{j \in \{\Phi_{b_1} \setminus b_0\}} [\exp(-\gamma_{th} x^\beta d_{u_0, b_j}^{-\beta} |h_{u_0, b_j}|^2)]\right\} \\ &\stackrel{(a)}{=} \exp\left\{-\lambda_{b_1} \int_{R^2 \setminus \mathcal{C}_{(u_0, x)}} \left[1 - \mathbb{E}_{|h_{u_0, b_j}|^2}(e^{-\gamma_{th} x^\beta r^{-\beta}})\right] dr\right\} \\ &\stackrel{(b)}{=} \exp\left[-2\pi\lambda_{b_1} \int_x^\infty \frac{v}{1 + (\gamma_{th} x^\beta)^{-1} v^\beta} dv\right] \\ &\stackrel{(c)}{=} \exp\left[-\pi\lambda_{b_1} x^2 \gamma_{th}^{\frac{2}{\beta}} \int_{\frac{-x}{\gamma_{th}^{\frac{1}{\beta}}}}^\infty \frac{dy}{1 + y^{\frac{\beta}{2}}}\right] \\ &= \exp[-\pi\lambda_{b_1} x^2 \mathcal{Z}(\gamma_{th})], \quad (25) \end{aligned}$$

where step (a) follows from the probability generating functional (PGFL) of PPP, step (b) is obtained by converting the cartesian coordinates into polar coordinates, step (c) is obtained by replacing $(\gamma_{th} x^\beta)^{-\frac{2}{\beta}} v^2$ with y .

Similarly, the Laplace transform of the $\mathcal{L}_{I_{\Phi_{b_3}}}$ is

$$\begin{aligned} \mathcal{L}_{I_{\Phi_{b_3}}}\left[\frac{\gamma_{th} x^\beta}{\theta}\right] &= \mathbb{E}_{I_{\Phi_{b_3}}}\left[\exp\left(-\frac{\gamma_{th} x^\beta}{\theta} \sum_{l \in \Phi_{b_3}} d_{u_0, b_l}^{-\beta} |h_{u_0, b_l}|^2\right)\right] \\ &= \exp\left[-\pi\lambda_{b_3} x^2 \mathcal{Z}\left(\frac{\gamma_{th}}{\theta}\right)\right]. \quad (26) \end{aligned}$$

By substituting (25), (26) into (24), we can obtain Lemma 1 and the proof is completed.

B. Proof of Lemma 2

Let us replace the distance d_{e_i, b_0} with x . When $\gamma_{ec} \leq \gamma_{th_0}$, by substituting (8) into (10), the CDF of γ_{ec} is

$$\begin{aligned} F_{\gamma_{ec}}(\gamma_{th}) &\triangleq P_r\left\{\max_{e_i \in \Phi_e} [SINR_{e_i} \leq \gamma_{th}]\right\} \\ &= P_r\left\{\max_{e_i \in \Phi_e} \left[\frac{\theta P |h_{e_i, b_0}|^2 d_{e_i, b_0}^{-\beta}}{P I_{\Phi_b} + \sigma^2 + (1-\theta)P |h_{e_i, b_0}|^2 d_{e_i, b_0}^{-\beta}} \leq \gamma_{th}\right]\right\} \\ &= \mathbb{E}_{\Phi_e} \left[\prod_{i \in \Phi_e} P_r\left(\frac{\theta P |h_{e_i, b_0}|^2 d_{e_i, b_0}^{-\beta}}{P I_{\Phi_b} + \sigma^2 + (1-\theta)P |h_{e_i, b_0}|^2 d_{e_i, b_0}^{-\beta}} \leq \gamma_{th}\right) \right] \\ &\stackrel{(a)}{=} \exp\left\{-\lambda_e \int_{R^2} 1 - P_r\left[|h_{e_i, b_0}|^2 \leq \frac{(P I_{\Phi_b} + \sigma^2) \gamma_{th} r^\beta}{[\theta - (1-\theta) \gamma_{th}] P}\right] dr\right\} \\ &\stackrel{(b)}{=} \exp\left\{-2\pi\lambda_e \int_0^\infty x \mathcal{L}_{I_{\Phi_b}}\left[\frac{\gamma_{th} x^\beta}{[\theta - (1-\theta) \gamma_{th}]}\right] e^{-\frac{\sigma^2 \gamma_{th} x^\beta}{[\theta - (1-\theta) \gamma_{th}] P}} dx\right\} \quad (27) \end{aligned}$$

where step (a) follows from the PGFL of PPP, step (b) is obtained by converting the cartesian coordinates into polar coordinates.

Note that the interference comes from $\{\Phi_b \setminus b_0\}$, which is the reduced Palm distribution of PPP Φ_b . According to Slivnyak-Mecke theorem [16], the reduced Palm distribution of PPP is equivalent of its original distribution, i.e. $\{\Phi_b \setminus b_0\} = \Phi_b$ as illustrated in [9]. Denoting $S = \frac{\gamma_{th} x^\beta}{[\theta - (1-\theta) \gamma_{th}]}$, the Laplace transform of interference $I_{\Phi_b}(S)$ is derived as

$$\begin{aligned} \mathcal{L}_{I_{\Phi_b}}(S) &= \mathbb{E}_{I_{\Phi_b}}[e^{-S I_{\Phi_b}}] \\ &= \mathbb{E}_{I_{\Phi_b}}\left[\exp(-S \sum_{j \in \{\Phi_b \setminus b_0\}} |h_{e_i, b_j}|^2 d_{e_i, b_j}^{-\beta})\right] \\ &\stackrel{(a)}{=} \exp\left\{-\lambda_b \int_{R^2} 1 - \mathbb{E}_{|h_{e_i, b_j}|^2} [\exp(-S |h_{e_i, b_j}|^2 d_{e_i, b_j}^{-\beta})] d(d_{e_i, b_j})\right\} \\ &\stackrel{(b)}{=} \exp\left\{-2\pi\lambda_b \int_0^\infty \frac{v}{1 + \frac{v^\beta}{S}} dv\right\} \\ &= \exp\left[-\pi\lambda_b \Gamma\left(1 + \frac{2}{\beta}\right) \Gamma\left(1 - \frac{2}{\beta}\right) S^{\frac{2}{\beta}}\right], \quad (28) \end{aligned}$$

where step (a) follows from the PGFL of PPP, where step (b) is obtained by converting cartesian coordinates into polar coordinates.

By substituting (28) into (27), we can get $\tilde{F}_{\gamma_{ec}}(\gamma_{th})$ as (15). When γ_{ec} is larger than γ_{th_0} , it is clearly to note that $F_{\gamma_{ec}}(\gamma_{th}) = 1$. Then the proof is completed.

REFERENCES

- [1] Y.-S. Shiu, S. Y. Chang, H.-C. Wu, S. C.-H. Huang, and H.-H. Chen, "Physical layer security in wireless networks: A tutorial," *IEEE Wireless Commun.*, vol. 18, no. 2, pp. 66–74, Apr. 2011.
- [2] A. D. Wyner, "The wire-tap channel," *Bell Syst. Tech. J.*, vol. 54, no. 8, pp. 1355–1387, 1975.
- [3] S. Goel and R. Negi, "Guaranteeing secrecy using artificial noise," *IEEE Trans. Wireless Commun.*, vol. 7, no. 6, pp. 2180–2189, June. 2008.
- [4] L. Dong, Z. Han, A. P. Petropulu, and H. V. Poor, "Improving wireless physical layer security via cooperating relays," *IEEE Trans. Signal Process.*, vol. 58, no. 3, pp. 1875–1888, Mar. 2010.
- [5] J. G. Andrews, F. Baccelli, and R. K. Ganti, "A tractable approach to coverage and rate in cellular networks," *IEEE Trans. Commun.*, vol. 59, no. 11, pp. 3122–3134, Nov. 2011.

- [6] X. Zhang, X. Zhou, and M. R. McKay, "Enhancing secrecy with multi-antenna transmission in wireless ad hoc networks," *IEEE Trans. Inf. Forensics Security*, vol. 8, no. 11, pp. 1802–1814, Nov. 2013.
- [7] H. Wang, X. Zhou, and M. C. Reed, "Physical layer security in cellular networks: A stochastic geometry approach," *IEEE Trans. Wireless Commun.*, vol. 12, no. 6, pp. 2776–2787, Jun. 2013.
- [8] Y. Deng, L. Wang, M. ElKashlan, A. Nallanathan, and R. K. Mallik, "Physical layer security in three-tier wireless sensor networks: A stochastic geometry approach," *IEEE Trans. Inf. Forensics Security*, vol. 11, no. 6, pp. 1128–1138, Jun. 2016.
- [9] W. Tang, S. Feng, Y. Ding, and Y. Liu, "Jammer selection in heterogeneous networks with full-duplex users," in *Global Commun. Conf. (GLOBECOM), 2016 IEEE*. IEEE, Feb. 2017, pp. 1–6.
- [10] H. Liu, Z. Chen, and L. Qian, "The three primary colors of mobile systems," *IEEE Commun. Mag.*, vol. 54, no. 9, pp. 15–21, Sep. 2016.
- [11] C. Yang, Y. Yao, Z. Chen, and B. Xia, "Analysis on cache-enabled wireless heterogeneous networks," *IEEE Trans. Wireless Commun.*, vol. 15, no. 1, pp. 131–145, Jan 2016.
- [12] A. Sengupta, R. Tandon, and T. C. Clancy, "Fundamental limits of caching with secure delivery," *IEEE Trans. Inf. Forensics Security*, vol. 10, no. 2, pp. 355–370, Feb. 2015.
- [13] C. Yang, B. Xia, W. Xie, K. Huang, Y. Yao, and Y. Zhao, "Interference cancellation at receivers in cache-enabled wireless networks," *IEEE Trans. Veh. Technol.*, Aug. 2017.
- [14] L. Xiang, D. W. K. Ng, R. Schober, and V. W. Wong, "Cache-enabled physical-layer security for video streaming in wireless networks with limited backhaul," in *GC Wkshps, 2016 IEEE*. IEEE, Feb 2017, pp. 1–7.
- [15] H. ElSawy, E. Hossain, and M. Haenggi, "Stochastic geometry for modeling, analysis, and design of multi-tier and cognitive cellular wireless networks: A survey," *IEEE Commun. Surveys & Tutorials*, vol. 15, no. 3, pp. 996–1019, June. 2013.
- [16] S. N. Chiu, D. Stoyan, W. S. Kendall, and J. Mecke, *Stochastic geometry and its applications*. John Wiley & Sons, 2013.